PERFORMANCE EVALUATION OF A WALKING BEAM TYPE REHEATING FURNACE BASED ON ENERGY AND EXERGY ANALYSIS

by

Wenjie RONG [a,b], ***Baokuan LI*** [a,b*], ***and Fengsheng QI*** [a,b]

[a] School of Metallurgy, Northeastern University, Shenyang, China
[b] Key Laboratory of Data Analytics and Optimization for Smart Industry (Northeastern University), Ministry of Education, Shenyang, China

Original scientific paper
https://doi.org/10.2298/TSCI200424226R

A walking beam type reheating furnace with advanced control technology has been evaluated by combined energy and exergy analysis. In order to gain insight into the performance of the present furnace, the results of energy analysis are compared with those in published papers and the irreversibility of the furnace is analyzed via exergy destruction calculation. The results show that slabs preheated before charged into the furnace can save fuel and improve energy utilization. The structure and material of the wall and roof show good thermal insulation. However, the oxidized scale is a little more and the temperature of flue gas is high in the present reheating furnace. The energy efficiency of the furnace is 71.01%, while exergy efficiency is 51.41%, indicating a potential for energy-saving improvements of the present furnace. The exergy destruction of the furnace accounts for 28.36% of total exergy input which is mainly caused by heat transfer through a finite temperature difference (14.71%), fuel combustion (11.66%), and scale formation (1.99%).

Key words*: walking beam type reheating furnace, energy analysis, exergy analysis, exergy destruction*

Introduction

About 23% of the annual energy consumption in China is caused by industrial furnace. Meanwhile, due to the strict environmental regulations and policies issued in recent years, it is particularly important to reduce the emissions of combustion pollutants in the furnace. Reheating furnace, which is the second-largest energy consumer and main emitter of greenhouse gases in steel enterprise, should be emphatically investigated. In our previous paper [1], pollutant control has been numerically investigated while the present paper will focus on energy efficiency assessment for the same reheating furnace. Reheating furnace is commonly used for heating slabs above the recrystallization temperature for plastic deformation before transported into a rolling mill [2, 3]. In current industry practice, there are several types of reheating furnaces; including the rotary hearth reheating furnace, the pusher-type reheating furnace and the walking beam type reheating furnace. Among all these reheating furnaces, the walking beam type reheating furnace has been widely used because of its high productivity and flexible control. Aiming to further boost the productivity quality of steel slabs, a series of walking beam type reheating furnaces have been designed and built.

* Corresponding author, e-mail: libk@smm.neu.edu.cn

Recently, numerous studies have been done on heating furnace [3-17]. Relatively thorough studies were carried out on the reheating furnace by Han *et al.* [3-8] from 2007 to 2012. They developed numerical programs to study slab heating characteristics and thermal efficiency of small and full-scale furnaces. On the other hand, oxy-fuel combustion, which is an alternative method to enhance the energy efficiency of the furnace, has been investigated [10-12]. About the thermal performance of reheating furnace, Pepe *et al.* [13] designed an advanced process control system to control and optimize a walking beam billets reheating furnace. Chen *et al.* [15] also investigated energy consumption and performance of reheating furnace by means of both numerical predictions and practical measurements. The proportion of energy recovery from flue gas via heat exchanger was more than 50%, so the heat exchanger played an important role in the energy management of reheating furnace. Nevertheless, the temperature of the flue gas exited from the heat exchanger was still high. Kangvanskol *et al.* [16] proposed a slab preheating chamber to further recover the energy of flue gas to preheat slabs before charged into the furnace. They reported that the fuel consumption reduced, and the energy efficiency increased due to the implementation of the slab preheating chamber. Moreover, several measures to improve efficiency were conducted in practice by Kilinc *et al.* [17] including reducing excess air, preventing air leakage loss of regenerator and establishing economizer. The efficiency of the reheating furnace was raised from 61.83-69.43% after the implementation of energy-saving measures.

An alternative way to evaluate the thermal efficiency of a reheating furnace is by means of exergy analysis. Luo *et al.* [18] established exergy balances for two reheating furnaces, one with cold slabs and anther one with preheated slabs. The exergy destruction of combustion which was the main exergy destruction of reheating furnace was mentioned but not calculated in detail. In addition, Xu *et al.* [19] presented an exergy assessment for a reheating furnace and proposed several suggestions for efficiency improvement. Although the energy and exergy of scale formation were considered, the exergy destruction caused by the chemical reaction of scale formation was neglected. Based on their researches, which have laid a firm foundation for a detailed exergy analysis of reheating furnace, the present work aims to develop an energy and exergy analysis model for evaluating the thermal performance of a walking beam type reheating furnace combined with exergy damage calculation.

Materials and method

Furnace structure and operating condition

The schematic diagram of the walking beam type reheating furnace can be found in [1]. This furnace, currently run in a steel enterprise, has an effective length of 51.7 m and a width of 11.7 m. The production rate was designed as 350 tonne per hour. The furnace wall, except for the part around the burners and holes, adopted a composite structure composed of castable, lightweight clay brick, and alumino-silicate fiber felt from inside to outside. Similarly, the furnace roof was composed of plastic materials, lightweight castable, alumino-silicate fiber insulation board and thermal insulation cream from inside to outside. The furnace was broadly divided into four zones along the heating process of slabs, namely, preheating zone, heating Zone I, heating Zone II, and soaking zone. Slabs are preheated in the preheat zone using the waste heat of flue gas and heated by absorbing heat of fuel combustion in other zones. There are 88 burners in the furnace, that is, a total of 30 flat burners are uniformly set on the top of the soaking zone and other 58 flame burners are set on the two sides of the furnace. Every zone is consisting of upper and lower heat supply sections. There are eight automatic control sections of furnace temperature which can be seen in fig. 1. In the reheating furnace, pieces of slabs were moved stepwise by walking beams after charged into the furnace, and then discharged when they satisfy the two requirements, namely, target temperature and temperature uniformity. The fuel of the reheating furnace was a mixture of blast furnace gas, coke oven gas, converter gas and natural gas (the composition of fuel by volume fraction is 0.2708 CO, 0.1404 H_2, 0.0772 CH_4, 0.0063 C_2H_4, 0.3491 N_2, 0.1457 CO_2, and 0.0104 O_2) [1].

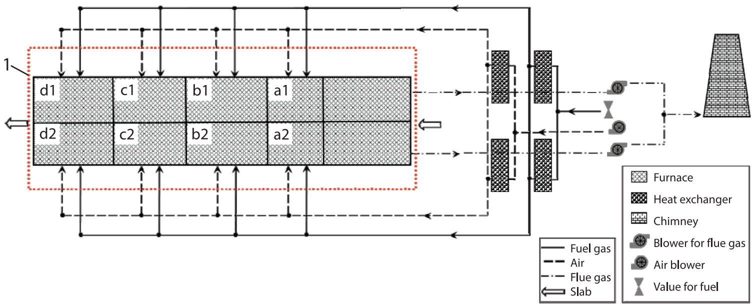

Figure 1. Flow diagram for gases in the walking beam type reheating furnace

As depicted in fig. 1, flue gas was led to pass through two sets of heat exchangers to recover the energy for preheating fuel and combustion air. The combustion air was taken from the ambient atmosphere. The initial temperature of the fuel is 312.15 K. The temperature of flue gas was measured with four thermocouples before and after the air heat exchangers and two thermocouples after the fuel heat exchangers. Thus, the temperatures of flue gas at different positions were easily obtained and the average temperature of the two sets of measurement data at the same position was used in the present analysis. In addition, the measured values of the slab mass-flow rate, scale loss and the temperatures of preheated fuel and combustion air were read from the system counters.

In the process of slab heating, metal is easy to react with thermal oxidation combustion gas (*i.e.* O_2, CO_2, H_2O, and N_2) in high temperature environment [20]. The equations of reaction are listed in eqs. (1)-(6) [20]. The reaction products, also called oxidized scale, are one of the important factors which have a direct influence on the surface quality of the steel, and the oxidation damage rate is a major index for evaluating reheating furnace. The scale yields a material loss, and the amount of material loss is related to furnace operating conditions such as steel temperature, excess combustion air, and steel residence time in the furnace [21]. The oxidized layer which forms on the slab surface is generally made up of wustite (FeO), magnetite (Fe_3O_4), and hematite (Fe_2O_3) from inside to outside. When the furnace temperature is higher than 873 K, the percent compositions of the three oxides, wustite, magnetite, and hematite are about 96%, 4%, and 1%, respectively [21]. Therefore, for simplicity, the scale layer is assumed to be wustite:

$$2Fe + O_2 = 2FeO \tag{1}$$

$$3Fe + 2O_2 = Fe_3O_4 \tag{2}$$

$$4Fe + 3O_2 = 2Fe_2O_3 \tag{3}$$

$$Fe + CO_2 = FeO + CO \tag{4}$$

$$3Fe + 4CO_2 = Fe_3O_4 + 4CO \tag{5}$$

$$Fe + H_2O = FeO + H_2 \tag{6}$$

Theoretical analysis

The theoretical analysis method adopted was described in detail in our previous two papers, and therefore, the basic equations will not be demonstrated here [22, 23]. Considering the complexity and instability of the walking beam type reheating furnace, several assumptions for thermodynamic assessment are made as follows [24-27]:

– Steady-state and steady flow conditions are assumed for the reheating furnace.
– The ambient and average surface temperatures are constant throughout the period of the study.
– The changes of kinetic and potential energy of input and output materials are negligible.
– Gas leakage in the reheating furnace is neglected.
– The principle of the ideal gas mixture is used for the gases inside the system.
– The temperature and pressure of the environmental state are set at T_0 = 298.15 K and P_0 = 1 atmosphere.

Based on the assumptions, a control volume is defined as shown in the red dotted frame – 1 in fig. 1. The input mass-flows consist of four terms, namely, preheated fuel, preheated combustion air, low temperature slabs, and cooling water. The high temperature slabs and flue gas are output mass-flows. In addition, the oxide scale is considered as a separate output mass-flow. Cooling water evaporates in skids, so steam is one of the output mass-flows (for making it consistent with energy and exergy flows, the subscript skl stands for the mass-flow of steam). The mass balance equation can be written:

$$\dot{m}_{\mathrm{f}} + \dot{m}_{\mathrm{ca}} + \dot{m}_{\mathrm{sl}} + \dot{m}_{\mathrm{cw}} = \dot{m}_{\mathrm{fg}} + \dot{m}_{\mathrm{sh}} + \dot{m}_{\mathrm{skl}} + \dot{m}_{\mathrm{sc}} \tag{7}$$

where the subscripts, f, and, ca, stand for fuel and combustion air, respectively. The subscripts, sl, and, sh, stand for the low and high temperature slabs, respectively. The subscripts, fg, and, sc, stand for flue gas and oxidized scale, respectively. The subscript, sw, stands for cooling water.

In the scale formation process, there will be a small part of O_2 consumed and the mass-flow rate of flue gas is calculated:

$$\dot{m}_{\mathrm{fg}} = \dot{m}_{\mathrm{f}} + \dot{m}_{\mathrm{ca}} - \dot{m}_{\mathrm{sc}} \frac{M_{\mathrm{O}}}{M_{\mathrm{FeO}}} \tag{8}$$

where M_{O} and M_{FeO} are molecular mass of oxygen and wustite, respectively. The result of mass balance is shown in tab. 1.

Table 1. Mass-flow balance

Input flows	Amount [kgh^{-1}]	Output flows	Amount [kgh^{-1}]
Fuel	12920	Flue gas	34424
Combustion air	22151	High temperature slabs	217442
Low temperature slabs	219705	Scale	2910
Cooling water	10500	Steam	10500
Total	265276	Total	265276

For the energy balance, fuel combustion is the main energy supply for the reheating furnace. The input energy flow of fuel is divided into physical energy and chemical energy [28]. The temperature of the preheated fuel is 465 K and the low heat value of fuel is 8096 kJ/m^3. In the present work, the combustion air is preheated to 633 K and its composition is defined as 77.48% N_2, 20.59% O_2, 1.90% H_2O, and 0.03% CO_2 [22]. It is reported that 0.017% CO residents in the flue gas, so the output energy flow of combustion includes not only the energy flow of flue gas but also the energy flow due to incomplete combustion. Slabs in the present reheating furnace are charged with a temperature higher than the ambient temperature (*i.e.* 506 K), so the slabs bring energy to the reheating furnace. After being heated, the high temperature slabs are discharged with certain energy. Additionally, although scale formation is unfavorable in a reheating furnace, the heat of chemical reaction has to be considered as an input flow of energy because the scale formation is an exothermic reaction.

Furthermore, the energy loss of the wall and roof is significant parts of energy output. As depicted in tab. 2, the furnace surface is divided into eight parts since the furnace temperatures are measured by eight thermocouples.The heat loss of the roof and wall can be calculated [29]:

$$\dot{E}n_1 = A\frac{T_{\text{fur}} - T_0}{\dfrac{1}{\alpha_{\text{fur}}} + \dfrac{L_{\text{n}}}{\lambda_{\text{n}}} + \ldots + \dfrac{L_2}{\lambda_2} + \dfrac{L_1}{\lambda_1} + \dfrac{1}{\alpha_0}} \tag{9}$$

where A is the area, L and λ are thicknesses and conductive coefficients of different layers, T_{fur} and T_0 – the furnace temperature and ambient temperature, respectively, α_{fur} and α_0 – the convective heat transfer coefficients inside and outside the wall or roof, respectively. In addition the loss from the wall and roof, the energy loss from the furnace door and hole shall be included in the furnace loss. However, considering that the parameters of the furnace door and furnace hole are not easy to obtain, the energy loss from these positions is included in other losses.

Table 2. Parameters of wall and roof in the walking beam type reheating furnace

Zone	Roof area [m^2]	Wall area [m^2]	Temperature [K]	Roof heat loss [kW]	Wall heat loss [kW]
Preheating zone A	166.18	93.49	1280.25	146.19	32.53
Heating zone I A	59.67	43.24	1434.15	114.50	29.61
Heating zone II A	50.90	36.94	1464.25	100.86	26.03
Soaking zone A	53.39	34.19	1407.75	100.20	22.95
Preheating zone B	166.18	93.49	1220.05	139.36	31.10
Heating zone I B	59.67	43.24	1428.45	114.38	29.58
Heating zone II B	50.90	36.94	1438.85	98.79	25.56
Soaking zone B	53.39	34.19	1400.75	99.97	22.90

Thus, the energy balance can be expressed:

$$\dot{E}n_{\text{f,c}} + \dot{E}n_{\text{f,s}} + \dot{E}n_{\text{ca}} + \dot{E}n_{\text{sl}} + \dot{E}n_{\text{scf}} = \dot{E}n_{\text{fg}} + \dot{E}n_{\text{sh}} + \dot{E}n_{\text{skl}} + \dot{E}n_{\text{sc,s}} + \dot{E}n_{\text{fl}} + \dot{E}n_{\text{ic}} + \dot{E}n_{\text{e}} \tag{10}$$

where $\dot{E}n_{\text{f,c}}$ and $\dot{E}n_{\text{f,s}}$ are the heat of fuel combustion and the sensible heat of fuel, respectively, $\dot{E}n_{\text{scf}}$ and $\dot{E}n_{\text{sc,s}}$ – the heat of chemical reaction of scale formation and the sensible heat of scale, respectively, and $\dot{E}n_{\text{skl}}$ – the skid loss including the sensible and latent heat of steam. The result of the energy balance is summarized in tab. 3.

Table 3. Energy flow balance

Input flows	T [K]	Amount [kW]	Output flows	T [K]	Amount [kW]
Fuel combustion	–	38622.79	Flue gas	818	6411.38
Sensible heat of fuel	465	1844.36	High temperature slabs	1502	36743.31
Sensible heat of combustion air	633	2182.76	Scale	1502	705.48
			Skid loss	–	6681.35
Low temperature slabs	506	6458.41	Furnace loss	–	1134.51
Scale formation	–	3014.56	Incomplete combustion	–	61.80
–	–		Other losses	–	385.05
Total	–	52122.88	Total	–	52122.88

Energy efficiency is defined as the ratio of the energy gained by slabs and the energy provided by preheated fuel and preheated combustion air:

$$\eta_{\text{en}} = \frac{\dot{E}n_{\text{sh}} - \dot{E}n_{\text{sl}}}{\dot{E}n_{\text{supply}}} \tag{11}$$

The exergy balance of the walking beam type reheating furnace includes the input flows of fuel, combustion air, and low temperature slabs and the output flows of flue gas, high temperature slabs, skid loss, scale, and furnace loss through the furnace surface:

$$\dot{E}x_{\text{f}} + \dot{E}x_{\text{ca}} + \dot{E}x_{\text{sl}} = \dot{E}x_{\text{fg}} + \dot{E}x_{\text{sh}} + \dot{E}x_{\text{skl}} + \dot{E}x_{\text{sc}} + \dot{E}x_{\text{fl}} + \dot{E}x_{\text{d}} \tag{12}$$

where $\dot{E}x_{\text{f}}$ includes physical and chemical exergy flows of fuel.

After the input and output exergy flows were determined, the total exergy destruction $\dot{E}x_{\text{d}}$, which is the difference between input and output exergy flows, can be obtained. In order to analyze exergy destructions, a detailed calculation of entropy generation is given first. In the present case, the sources of entropy generation are determined as three terms: fuel combustion, scale formation and heat transfer through a finite temperature difference. It is worth mentioning that the scale formation process is an exothermic reaction, so the heat generated in the reaction is an input energy flow in energy analysis. However, the irreversible reaction in exergy analysis leads to entropy generation, so the scale formation is a part of exergy destruction in exergy analysis. The slabs being heated is a typical heat transfer through a finite temperature difference between furnace gas and slabs. The exergy destruction calculation can be expressed as:

$$\dot{E}x_{\text{d}} = \dot{E}x_{\text{d,c}} + \dot{E}x_{\text{d,scf}} + \dot{E}x_{\text{d,ht}} \tag{13}$$

where $\dot{E}x_{\text{d,c}}$, $\dot{E}x_{\text{d,cf}}$, and $\dot{E}x_{\text{d,ht}}$ and are exergy destruction as a result of combustion, exergy destruction due to scale formation and exergy destruction caused by heat transfer through a finite temperature difference, respectively.

The entropy generation of fuel combustion is shown in tab. 4. The enthalpy values for CH_4 and C_2H_4 can be found in [30] and the entropy and enthalpy values for other components can be found in [31]. Entropy generation of the scale formation is shown in tab. 5. Then, the exergy destruction of fuel combustion and the exergy destruction of scale formation are determined. The exergy destruction of heat transfer through a finite temperature difference is calculated as the difference between the total exergy destruction, calculated in the exergy balance, and the sum of the exergy destruction due to combustion and scale formation. The exergy balance results are summarized in tab. 6.

Exergy efficiency is determined consistent with energy efficiency:

$$\eta_{ex} = \frac{\dot{E}x_{sh} - \dot{E}x_{sl}}{\dot{E}x_{supply}} \tag{14}$$

Table 4. Entropy generation of fuel combustion

	Mass [kg]	n_i [kmol]	s [kJkmol^{-1}K^{-1}]	x_i	$-R\ln(x_i \cdot P)$	$n_i s_i$ [kJkg^{-1}K^{-1}]	h [kJmol^{-1}]
Fuel							
CO	0.2938	$1.05 \cdot 10^{-2}$	210.18	$2.71 \cdot 10^{-1}$	10.87	2.32	–105.57
H_2O	0.0005	$2.66 \cdot 10^{-5}$	203.38	$6.87 \cdot 10^{-4}$	60.55	0.01	–236.04
O_2	0.0130	$4.05 \cdot 10^{-4}$	217.97	$1.04 \cdot 10^{-2}$	37.93	0.10	5.04
N_2	0.3787	$1.35 \cdot 10^{-2}$	204.08	$3.49 \cdot 10^{-1}$	8.76	2.88	4.94
CO_2	0.2484	$5.65 \cdot 10^{-3}$	231.34	$1.46 \cdot 10^{-1}$	16.02	1.40	–386.49
H_2	0.0109	$5.44 \cdot 10^{-3}$	142.90	$1.40 \cdot 10^{-1}$	16.33	0.87	4.83
CH_4	0.0479	$2.99 \cdot 10^{-3}$	203.64	$7.71 \cdot 10^{-2}$	21.30	0.67	–79.87
C_2H_4	0.0069	$2.45 \cdot 10^{-4}$	241.72	$6.33 \cdot 10^{-3}$	42.09	0.07	47.54
Combustion air							
O_2	0.5559	$1.74 \cdot 10^{-2}$	228.08	$2.06 \cdot 10^{-1}$	13.14	4.19	10.40
N_2	1.8304	$6.54 \cdot 10^{-2}$	213.74	$7.75 \cdot 10^{-1}$	2.12	14.11	10.01
CO_2	0.0011	$2.53 \cdot 10^{-5}$	245.95	$3.00 \cdot 10^{-4}$	67.44	0.01	–378.79
H_2O	0.0289	$1.60 \cdot 10^{-3}$	214.86	$1.90 \cdot 10^{-2}$	32.95	0.40	–230.01
Products							
CO_2	0.8632	$1.96 \cdot 10^{-2}$	309.95	$1.70 \cdot 10^{-1}$	14.72	6.37	–298.81
N_2	2.2091	$7.89 \cdot 10^{-2}$	252.73	$6.85 \cdot 10^{-1}$	3.15	20.19	57.72
H_2O	0.2438	$1.35 \cdot 10^{-2}$	265.56	$1.18 \cdot 10^{-1}$	17.80	3.84	–166.94
O_2	0.1001	$3.13 \cdot 10^{-3}$	269.24	$2.72 \cdot 10^{-2}$	29.98	0.94	60.74
CO	0.0001	$4.20 \cdot 10^{-6}$	259.29	$3.64 \cdot 10^{-5}$	84.97	0.00	–52.35
ΔS [kJkg^{-1}K^{-1}]						4.31	
q_r [kJmol^{-1}]							407.58

Table 5. Entropy generation of scale formation

	n [kmol]	S [kJkmol^{-1}K^{-1}]	h [kJmol^{-1}]
Reactants			
Fe	2	60.49	18.79295
O_2	1	238.56	18.27915
Products			
FeO	2	118.34	–240.62505
ΔS [kJkmol^{-1}K^{-1}]		–122.849	
q_r [kJmol^{-1}]			537.115

Table 6. Exergy flow balance

Exergy input [kW]		Exergy output [kW]		Exergy destruction [kW]	
Fuel	39039.95	Flue gas	4064.78	Combustion	4825.12
Combustion air	785.00	Skid loss	2873.09	Scale formation	823.97
Low temperature slabs	1556.33	High temperature slabs	22029.95	Heat transfer through a finite temperature difference	6088.27
–		Scale	422.98	–	
–		Furnace loss	253.11	–	
Total	41381.28	Total	29643.92	Total	11737.36

Results and discussion

Energy analysis results

In order to gain insight into the current analysis results, a comparison of energy analysis results is made with those in literature as shown in tab. 7. It should be noted that the same type of furnace is used in the present paper [3, 6, 7, 32], but the structures of the furnaces are slightly different.

Table 7. Comparison of energy analysis results with those in literature

Data sources	Fuel energy flow [%]	Scale formation [%]	Wall loss [%]	Scale [%]	Energy efficiency [%]
Present paper	77.64	5.78	2.18	1.35	71.01
[3]	84.4	–	2.5	–	43.7
[6]	83.83	–	–	–	46.1
[7]	82.8	–	2.5	–	47.5
[32]	83.4	–	5.4	–	54.7
[16][a]	82.24	4.83	3.44	1.06	69.9
[16][b]	77.47	–	–	–	70.5

a – slabs were charged with ambient temperature and b – slabs were preheated before charged into the furnace

The energy flow of fuel accounts for 77.64% of the total energy input, which is lower than those reported in [3, 6, 7, 32]. The energy efficiency of the furnace is found to be 71.01%, which is higher than the results in cited studies. The benefit of preheated slabs has also been confirmed by Kangvanskol *et al.* [16]. Therefore, the comparison helps to validate the calculation results and proves the advantage of preheated slabs in the current reheating furnace. Moreover, as shown in fig. 2, the energy loss from the furnace surface (*i.e.* 2.18%) is lower compared with those in [3, 7, 16, 32] which shows a good insulation situation of the present walking beam type reheating furnace. Moreover, the energy flow of skid loss accounts for 12.82% which is closer to that in [7]. The energy of the steam exited from the skids has been recovered for power generation.

On the other hand, the scale formation as a separate input energy flow occurs in the present paper and [16]. Compared with their results, the energy flow due to scale formation in the present reheating furnace is slightly higher. The output energy flow of scale is also more than that in [16]. Therefore, the scale formation should be controlled in the present reheating

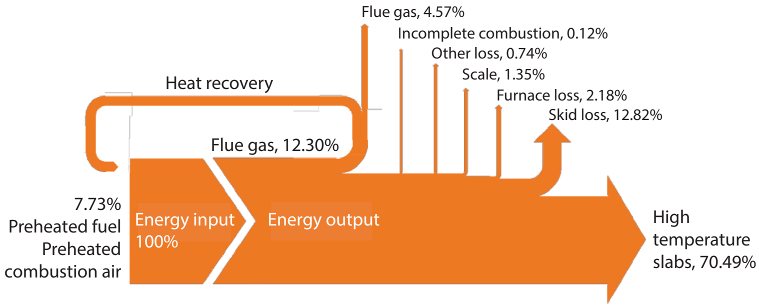

Figure 2. Sankey diagram for the walking beam type reheating furnace

furnace. The flue gas still has a temperature of 534 K after passing through the heat exchangers. Therefore, the heat recovery via heat exchangers needs to be further enhanced.

Exergy analysis results

The exergy balance results show that the main exergy source is the exergy flow of fuel, *i.e.* 94.34%, and the main exergy output flow is exergy flow of high temperature slabs, *i.e.* 53.24%. The exergy efficiency, 51.41%, of the walking beam type reheating furnace is lower than energy efficiency which indicates a potential for energy-saving.

Furthermore, the exergy destruction of the present walking beam type reheating furnace accounts for 28.36% of the total exergy input. The main exergy destruction is caused by heat transfer through a finite temperature difference, *i.e.* 14.71%. This part of exergy destruction is mostly due to the heat transfer between slabs and high temperature furnace gases. To reduce this exergy destruction, Luo *et al.* [18] mentioned two technologies. One is preheating the slabs before charged into the furnace, which has been implemented in the present case and another one is to use oxy-fuel combustion instead of air-fuel combustion. As mentioned in the introduction, oxy-fuel combustion has been used in reheating furnace in some works and its advantage has been confirmed.

On the other hand, exergy is also destroyed during the heat transfer process in the heat exchangers. It can be seen in fig. 2, the energy recovered from flue gas via heat exchangers accounts for 7.73% of the total energy input which corresponds to 62.84% of the total energy flow of flue gas. However, as depicted in fig. 3, the exergy recovery via heat exchangers accounts

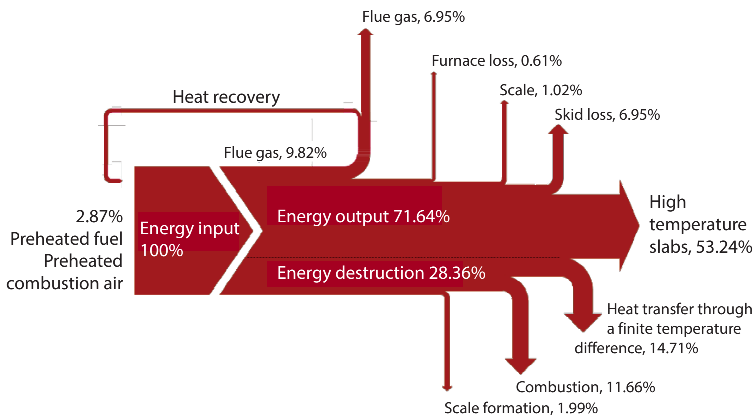

Figure 3. Grassmann diagram for the walking beam type reheating furnace

for 2.87% of the total exergy input, corresponding to 29.23% of the total exergy flow of flue gas which is much lower than that of energy recovery. Combined with energy analysis, the heat exchangers used in the current reheating furnace should be improved.

In addition, the exergy destruction due to combustion is 11.66% of the total exergy input. Once the heat exchangers are improved, this exergy damage could be reduced by preheating the fuel and combustion air at higher temperatures. Additionally, if the oxy-fuel combustion technology was applied, this exergy destruction would be lower.

Therefore, there are two directions for the improvement of the current heating furnace: the improvement of heat exchanger or the application of oxy-fuel combustion. However, the application of oxy-fuel leads to lower flue gas temperature compared with air-fuel combustion due mainly to the absence of nitrogen [9], which means if the oxy-fuel combustion was applied, then it may not be necessary to change the heat exchangers. Therefore, this paper can only put forward improvement suggestions for the current heating furnace. In the actual improvement measures, investment and effect should be considered comprehensively.

Furthermore, the exergy destruction of scale formation is 1.99% of the total exergy input. Combined with energy analysis, for the current reheating furnace, the oxidized scale can be reduced by increasing the preheat temperature of combustion air so as to decrease the residence time of the slabs. Thus, improving heat exchangers would also help the reduction of scale formation.

Conclusions

In this paper, a walking beam type reheating furnace was evaluated both from energy and exergy point of view. The main conclusions are summarized below.

- The energy efficiency of the walking beam type reheating furnace is 71.01%, while exergy efficiency is 51.41%, indicating a potential for energy-saving improvements.
- Compared with the results of energy analysis in several published studies, slabs preheated before charged into the furnace can save fuel and improve energy utilization. The structures and materials of the wall and roof showed good thermal insulation. However, the oxidized scale is a little more and the temperature of flue gas is high in this reheating furnace.
- The exergy destruction caused by heat transfer through a finite temperature difference, fuel combustion and scale formation is 14.71%, 11.66%, and 1.99% of the total exergy input, respectively.
- Combined energy and exergy analyses, the heat exchangers in the present walking beam type reheating furnace need to be improved. If the energy of flue gas could be further recovered to preheat fuel and combustion air, this furnace will be operated at higher energy efficiency. Moreover, to reduce the exergy destruction caused by heat transfer through a finite temperature difference, oxy-fuel combustion is an alternative method for the present reheating furnace.

Acknowledgment

The authors' gratitude goes to the National Natural Science Foundation of China (Grant No. 51934002) and the National Key R and D Program of China (2017YFB0304000) to support this research.

Nomenclature

A – area, [m^2]
$\dot{E}n$ – energy rate, [kJh^{-1}]
$\dot{E}x$ – exergy rate, [kJh^{-1}]
L – thickness, [m]
$\dot{m}$ – mass rate, [kgh^{-1}]
T – temperature, [°C]

Greek symbols

α – heat transfer coefficients
η – efficiency, [%]
λ – conductive coefficient, [Wm^{-1}K^{-1}]

Subscripts

c – combustion
ca – combustion air
cw – cooling water
d – destruction
e – test error
ex – exergy
f – fuel
fg – flue gas
fl – furnace loss
fur – furnace
ht – heat transfer
ic – incomplete combustion
n – number of layers
s – sensible heat
sc – scale
scf – scale formation
sh – high temperature slabs
skl – skid loss
sl – low temperature slabs
0 – ambient

References

[1] Qi, F., *et al*., Numerical Study on Characteristics of Combustion and Pollutant Formation in a Reheating Furnace, *Thermal Science*, *22* (2018), 5, pp. 2103-2112
[2] Hsieh, C. T., *et al*., A Numerical Study of Skid Marks on the Slabs in a Walking-Beam Type Slab Reheating Furnace, *Numerical Heat Transfer Part A Applications*, *57* (2010), 1, pp. 1-17
[3] Han, S. H., *et al*., Optimum Residence Time Analysis for a Walking Beam Type Reheating Furnace, *International Journal of Heat and Mass Transfer*, *55* (2012), 15-16, pp. 4079-4087
[4] Han, S. H., *et al*., Numerical Analysis of Heating Characteristics of a Slab in a Bench Scale Reheating Furnace, *International Journal of Heat and Mass Transfer*, *50* (2007), 9-10, pp. 2019-2023
[5] Han, S. H., *et al*., Transient Radiative Heating Characteristics of Slabs in a Walking Beam Type Reheating Furnace, *International Journal of Heat and Mass Transfer*, *52* (2009), 3-4, pp. 1005-1011
[6] Han, S. H., *et al*., A Numerical Analysis of Slab Heating Characteristics in a Walking Beam Type Reheating Furnace, *International Journal of Heat and Mass Transfer*, *53* (2010), 19-20, pp. 3855-3861
[7] Han, S. H., *et al*., Efficiency Analysis of Radiative Slab Heating in a Walking-Beam-Type Reheating Furnace, *Energy*, *36* (2011), 2, pp. 1265-1272
[8] Han, S. H., *et al*., Radiative Slab Heating Analysis for Various Fuel Gas Compositions in an Axial-Fired Reheating Furnace, *International Journal of Heat and Mass Transfer*, *55* (2012), 15-16, pp. 4029-4036
[9] Hu, Y., *et al*., Modelling and Simulation of Steel Reheating Processes under Oxy-Fuel Combustion Conditions-Technical and Environmental Perspectives, *Energy*, *185* (2019), Oct., pp. 730-743
[10] Prieler, R., *et al*., Numerical Analysis of the Transient Heating of Steel Billets and the Combustion Process under Air-Fired and Oxygen Enriched Conditions, *Applied Thermal Engineering*, *103* (2016), June, pp. 252-263
[11] Prieler, R., *et a*l., Prediction of the Heating Characteristic of Billets in a Walking Hearth Type Reheating Furnace Using CFD, *International Journal of Heat and Mass Transfer*, 92 (2012), Jan., pp. 675-688
[12] Mayr, B., *et al*., The CFD Modelling and Performance Increase of a Pusher Type Reheating Furnace Using Oxy-Fuel Burners, *Energy Procedia*, *120* (2017), Aug., pp. 462-468
[13] Pepe, C., *et al*., Energy Saving and Environmental Impact Decreasing in a Walking Beam Reheating Furnace, *Proceedings*, (C. A. Brebbia, Energy Production and Management in the 21st Century II), 2nd International Conference on Energy Production and Management, Ancona, Italy, 2016, Vol. 205, pp. 135-146
[14] Casal, J. M., *et al*., New Methodology for CFD 3-D Simulation of a Walking Beam Type Reheating Furnace in Steady-State, *Applied Thermal Engineering*, *86* (2015), July, pp. 69-80
[15] Chen, W. H., *et al*., Analysis on Energy Consumption and Performance of Reheating Furnaces in a Hot Strip Mill, *International Communications in Heat & Mass Transfer*, *32* (2005), 5, pp. 695-706
[16] Kangvanskol, K., *et al*., An Energy Analysis of a Slab Preheating Chamber for a Reheating Furnace, *Engineering Journal*, *18* (2014), 2, pp. 1-12

[17] Kilinc, E., *et al*., An Energy Efficiency Analysis of an Industrial Reheating Furnace and an Implementation of Efficiency Enhancements Methods, *Energy Exploration & Exploitation*, *32* (2014), 6, pp. 989-1003
[18] Luo, G., *et al*., Discussion of the Energy Saving Potential of Steel Reheating Furnace Based on Exergy Analysis (in Chinese), *Energy for Metallurical Industry*, *29* (2010), 2, pp. 46-48
[19] Xu, F., *et al.*, The Energy-Saving Technology on the Basis of Analysis of Heat and Exergy Balance for Heating Furnace (in Chinese), *Industrial Heating*, *34* (2005), 5, pp. 33-36
[20] Jang, J. H., *et al*., Investigation of the Slab Heating Characteristics in a Reheating Furnace with the Formation and Growth of Scale on the Slab Surface, *International Journal of Heat and Mass Transfer*, *53* (2010), 19-20, pp. 4326-4332
[21] Liu, X., *et al*., Numerical Simulation of Heat Transfer and Scale Formation in a Reheat Furnace, *Steel Research International*, *90* (2019), Oct., pp. 1-10
[22] Rong, W., *et al*., Energy and Exergy Analysis of an Annular Shaft Kiln with Opposite Burners, Applied *Thermal Engineering*, *119* (2017), June, p. 629-638
[23] Rong, W., *et al*., Exergy Assessment of a Rotary Kiln-Electric Furnace Smelting of Ferronickel Alloy, *Energy*, *138* (2017), July, pp. 942-953
[24] Sogut, M. Z., *et al*., Energetic and Exergetic Assessment of a Trass Mill Process in a Cement Plant, *Energy Conversion and Management*, *50* (2009), 9, pp. 2316-2323
[25] Odibi, C., *et al*., Exergy Analysis of a Diesel Engine with Waste Cooking Biodiesel and Triacetin, *Energy Conversion and Management*, *198* (2019), Oct., pp. 111912
[26] Zhang, Y., *et al*., Energy and Exergy Analyses of a Mixed Fuel-Fired Grate-Kiln for Iron Ore Pellet Induration, *Energy Conversion and Management*, *52* (2011), 5, pp. 2064-2071
[27] Ishaq, H., *et al*., Exergy Analysis and Performance Evaluation of a Newly Developed Integrated Energy System for Quenchable Generation, *Energ*y, *179* (2019), May, pp. 1191-1204
[28] Gurturk, M., *et al*., Energy and Exergy Analysis of a Rotary Kiln Used for Plaster Production, *Applied Thermal Engineering*, *67* (2014), 1-2, pp. 554-565
[29] Shi, L., Application and Discussion of Energy Saving Technology of Heating Furnace Body (in Chinese), *Modern Industrial Economy and Informationization*, *44* (2013), Mar., pp. 66-67
[30] Shi, X., *et al*., Heat Capacity and Formation Enthalpy of 700 Major Organic Compounds (in Chinese), *Chemical Engineering*, *17* (1989), 5, pp. 39-63
[31] Wu, Y., Che, Y., *Handbook of Inorganic Thermodynamic Data* (in Chinese), Northeastern University Press, Shenyang, China, 1993
[32] Morgado, T., *et al*., Assessment of Uniform Temperature Assumption in Zoning on the Numerical Simulation of a Walking Beam Reheating Furnace, *Applied Thermal Engineering*, *76* (2015), Feb., pp. 496-508

Paper submitted: April 24, 2020
Paper revised: July 14, 2020
Paper accepted: July 15, 2020